Therapeutics and Clinical Risk Management Dovepress

Open Access Full Text Article ORIGINAL RESEARCH

Endoscopic Endonasal Surgery of Skull Base Osteoradionecrosis with the Internal Carotid Artery Invaded: Clinical Characteristic and Surgical Strategy

Tianfeng Zhao[1], Zhuo Xu[2], Min Xu[2], Yubin Lai[2], Xiaodong Chen[2], Zhaohui Shi[3,4]

[1]Department of Otolaryngology-Head and Neck Surgery, General Hospital of Southern Theatre Command, Guangzhou, People's Republic of China; [2]Department of Otolaryngology-Head and Neck Surgery, Xijing Hospital, Air Force Military Medical University, Xi'an, People's Republic of China; [3]Department of Otolaryngology, Shenzhen Longgang Otolaryngology Hospital & Shenzhen Otolaryngology Research Institute, Shenzhen, People's Republic of China; [4]Department of Otolaryngology-Head and Neck Surgery, Naso-Orbital-Maxilla and Skull Base Center, Department of Allergy, the Third Affiliated Hospital of Sun Yat-Sen University, Guangzhou, People's Republic of China

Correspondence: Zhaohui Shi, Department of Otorhinolaryngology-Head and Neck Surgery, Naso-Orbital-Maxilla and Skull Base Center, Department of Allergy, Third Affiliated Hospital of Sun Yat-sen University, No. 600 Tianhe Road, Tianhe District, Guangzhou, Guangdong, 510630, People's Republic of China, Tel +86-20-85253333, Fax +86-20-85253336, Email shizhh35@mail.sysu.edu.cn

Objective: This study aims to summarize the clinical characteristics of skull base osteoradionecrosis (ORN) with the internal carotid artery (ICA) involvement and to distill the key surgical techniques that can enhance the protective measures for ICA.

Methods: We conducted a retrospective, observational study over a six-year period from February 2017 to May 2023. We included patients who were diagnosed with osteoradionecrosis with invasion of the internal carotid artery and collected their demographic information, pathology results, complication rates, ect. The goal was the alleviated rate after the surgery and the anatomic consideration during the surgery. We compared the verbal rating score (VRS) of headache pre- and post-operation by the Wilcoxon rank-sum test.

Results: A retrospective analysis was conducted on 19 patients diagnosed with ORN, with a mean age of 53.73 yr (range, 32–68 yr). Among them, 17 patients (89.47%) were nasopharyngeal carcinoma (NPC), 1 patient (5.23%) was squamous cell carcinoma of the sphenoid sinus, and 1 patient (5.23%) had adenoid cystic carcinoma. After the surgery, 1 fatality occurred within 2 months, which was attributed to a severe parapharyngeal space infection.1 patient succumbed to ICA rupture two days post-operation. Additionally, 1 patient experienced ORN recurrence 2 years after the initial surgery. The mean follow-up period for the study was 37.47 mo (range 2 −77 mo). The alleviation rate was 89.4%. The results revealed a significant decrease in VRS after the surgery (Z=−3.921, P=0.000). Finally, we summarized clinical evidences of ICA involvement, such as the formation of pseudoaneurysm.

Conclusion: A four-quadrant division of SBORN as a standardized and systematic approach is meaningful to guide surgical intervention for osteoradionecrosis. There are relevant clinical and imaging evidences that can predict the rupture of ICA.

Keywords: skull base osteoradionecrosis, skull base debridement surgery, endonasal endoscopic approach

Introduction

Skull base osteoradionecrosis (SBORN), a long-term complication resulting from radiotherapy for malignant tumors in the rhino-sinuses and nasopharynx, persists as a potentially life-threatening challenge with an incidence of 1–10%.[1] Radiotherapy induces hypo-vascularity, hypoxia, and hypocellularity, leading to the development of ORN.[2] Recent advancements in intensity-modulated radiotherapy and prophylactic management strategies have significantly reduced the morbidity associated with ORN.[3–7] Approximately 90% of cranial ORN cases occur in the mandible, a condition referred to as dental-extraction-related ORN.[2] However, for patients receiving radiotherapy for malignant tumors in nasopharynx, the skull base regions, including the palatine, vomer, sphenoid bone, clivus in the occipital bone, and the

Received: 25 May 2024
Accepted: 17 October 2024
Published: 19 December 2024

petrous apex in the temporal bone, are particularly susceptible to this damage. The onset of necrosis in these areas can result in lateral invasion of the parapharyngeal space, anterior extension into the planum sphenoidale and sella turcica, and posterior destruction of the atlanto-axial joint structure,[8,9] which is the main cause of poor prognosis.

Both conservative treatments and surgical interventions can effectively mitigate the risks associated with SBORN. Medical therapies, such as Pentoclo (a combination of tocopherol, pentoxifylline, and clodronate), emphasize the importance of antioxidant and antifibrotic agents in managing the condition. But in cases where medical treatment is ineffective, especially in instances involving ICA, surgical intervention remains the definitive solution. Compared to mandible ORN, SBORN is less well understood, owing primarily to its lower incidence rate.[10–15] Furthermore, the complexities and potential risks associated with ORN invading ICA pose significant challenges, including life-threatening hemorrhage, pseudoaneurysm, and blow-out carotid Blowout Syndrome (CBS).

In light of these challenges, the purpose of the manuscript is to develop a four-quadrant division approach for SBORN surgery with ICA involvement (Figure 1). This methodological framework can provide a systematic, reproducible, and step-wise surgical procedure that relies on anatomical landmarks for the management of SBORN.

Materials and Methods

The eligibility criteria were as follows: patients who had been diagnosed with SBORN, and patients in whom any segment of ICA was invaded and exposed during the surgical procedure, individuals who had a history of radiation and chemotherapy treatment for their primary tumor and presented no evidence of tumor recurrence, and patients who were suitable candidates for endoscopic endonasal debridement surgery. However, patients with a prior diagnosis of SBORN but confirmed tumor recurrence were disqualified. Additionally, patients who adopt a palliative surgical strategy or receive local anesthesia are also excluded.

After applying these criteria, a total of 20 patients were diagnosed with SBORN. Among them, 19 patients were included in this survey. The diagnosis of SBORN was based on the clinical presentation, medical history, computed tomography (CT) scan, magnetic resonance imaging (MRI), transnasal endoscopic examination, and pathological results.[16] All patients were subject to follow-up assessments 1 month after surgery, and then at regular intervals of 3 months for the first year after surgery, and 6 months thereafter. We compiled data on age, sex, tumor histopathology, TNM staging classification and clinical stage, post-radiotherapy complications, surgical approach, reconstruction technique, and survival time.

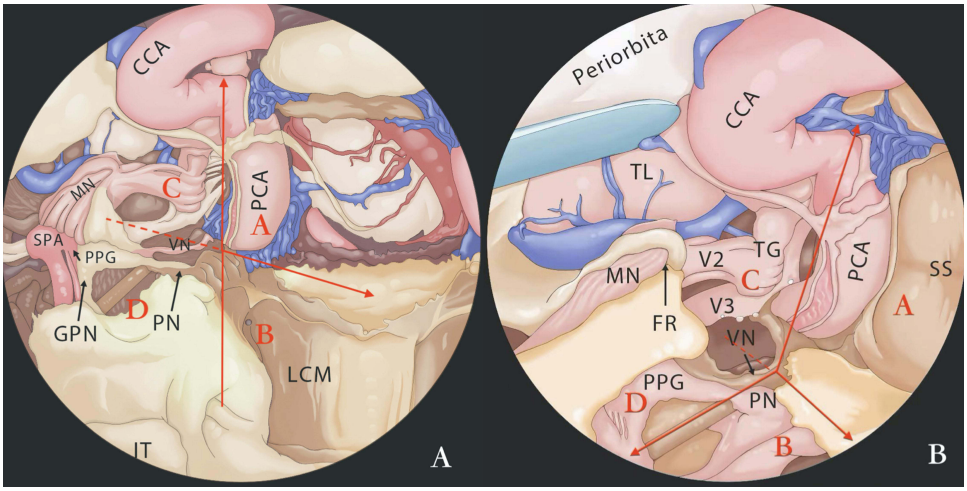

Figure 1 Schematic diagram of anatomical structure: The figure shows the surgical field is divided into four parts by the intersection of the horizontal segment of the internal carotid artery and the paraclival segment of the internal carotid artery (PCA) at the lacerum foramen and the pterygoid canal nerve (VN).

Notes: (**A** and **B**) Illustration of the division of the surgical field into four distinct parts based on the intersection of the horizontal segment of the internal carotid artery and the paraclival segment of the internal carotid artery (PCA) at the lacerum foramen and the pterygoid canal nerve (VN). Part (**B**) provides an enlarged view of part (**A**) for improved clarity. In part (**B**), some parts of the nasopharyngeal mucosa have been removed to expose the underlying structures in greater detail.

Abbreviations: ET, eustachian tube;V3, mandibular nerve; V2, maxillary nerve; SS, sphenoid sinus; PN, The pharyngeal nerve; PPG, the pterygopalatine ganglion; FR, Foramen rotundum; IT, inferior turbinate; LCM, longus capitis muscle; PCA, paraclival carotid artery; CCA, cavernous carotid artery; GPN, greater petrosal nerve; MN, maxillary nerve; TL, the temporal lobe; TG, trigeminal ganglion; FL, Foramen lacerum.

We employed ICA classification system:[17] (1) parapharyngeal segment (2) petrous segment (3) paraclival segment (4) parasellar segment (5) paraclinoid segment (6) intradural segment, then located ICA by CT or magnetic resonance imaging (MRI), with confirmation under endoscopic view.

The primary objectives were to assess the alleviated rate and to evaluate patient recovery status. We utilized the Verbal Rating Score (VRS) to evaluate the degree of headache experienced by patients both before and one week after surgery. The VRS consists of a 4-point scale with descriptive phrases ranging from "no pain" to "intense pain". Respondents were asked to select the single phrase that best characterized their level of pain intensity, providing a clear and objective measure of pain relief following surgery.[18]

All the advantages and adverse side effects after the surgery were part of the informed-consent discussion with patients and their families before surgery. All clinical records from the study were reviewed by the Ethics Committee of Longgang ENT Hospital. (SZLGENTEC2022-0224). Our research was in line with the Declaration of Helsinki.

Debridement Surgery

The patient was positioned in a supine position and administered general anesthesia. Following a revised prelacrimal recess approach, the medial wall of the maxillary sinus was carefully removed to expose the surgical site.[19,20] Subsequently, the anterior and posterior ethmoid sinus were opened, and either a nasal septal flap or lateral nasal wall flap was preserved for reconstruction.[21] Next, the pterygopalatine fossa (PPF) was exposed, and the vidian nerve was traced in a ventral-dorsal direction to the foramen lacerum. At this point, the petrous part of ICA was observed as it transitioned into the paraclival part. To gain access to ICA, necrotic bone was carefully drilled away, and the root of the pterygoid process was removed to expose the parapharyngeal space. Finally, a pedicled nasal septal flap was used to cover the surgical site and protect the exposed ICA. Following surgical intervention, patients received routine nasal irrigation and oral antibiotic treatment to promote healing.

In the context of the surgical approach, we have delineated the operative field into four quadrants. This segmentation is centered around the horizontal segment of ICA as it courses through the carotid canal, using the vidian nerve (VN) and the Lacerum foramen as central reference points (Figure 1).

Region A encompasses the paraclival segment of ICA. This area is situated adjacent to the VN inferiorly and abuts the parasellar ICA superiorly. Medially, it is bordered by the sellar region, while laterally, it is flanked by the maxillary nerve and the floor of the middle cranial fossa. The optic nerve and the optic-carotid recess (OCR) serve as critical anatomical landmarks for localization within this region.

Region B is positioned in the inferomedial quadrant of the operative field. Here, the VN serves as a critical marker for the exposure of the Lacerum foramen and subsequent localization of ICA. This area allows for safe operative maneuvers. Key anatomical structures within Region B include the petroclival fissure, the jugular foramen, and the hypoglossal foramen, each of which is integral to the surgical approach. (Figure 2).

Region C is infrequently affected, primarily due to its positioning in the relatively safe zone of the middle cranial fossa. Specifically, the area lateral to the maxillary nerve (V2) is considered safe for surgical intervention, minimizing the risk of compromising critical structures.

Region D (Figure 3) encompasses the eustachian tube, with key anatomical landmarks progressing from medial to lateral as follows: the vidian nerve (VN), the mandibular strut, the mandibular nerve (V3), and the external foramen of the carotid canal. The stratification from superficial to deep layers in this region includes the the levator veli palatini muscle, the mandibular nerve, a layer of fat tissue situated between the levator veli palatini (LVPM) and tensor veli palatini muscle (TVPM), and the parapharyngeal space. Laterally, this region is bounded by the carotid foramen and the parapharyngeal segment of ICA. Additional anatomical landmarks in this area include the mandibular nerve, the mandibular column, and the area below the inferior petrous apex. The region located inferior to ICA and anterior to the eustachian tube is deemed safe for surgical procedures, thereby reducing the likelihood of iatrogenic injury in these interventions (Table 1).

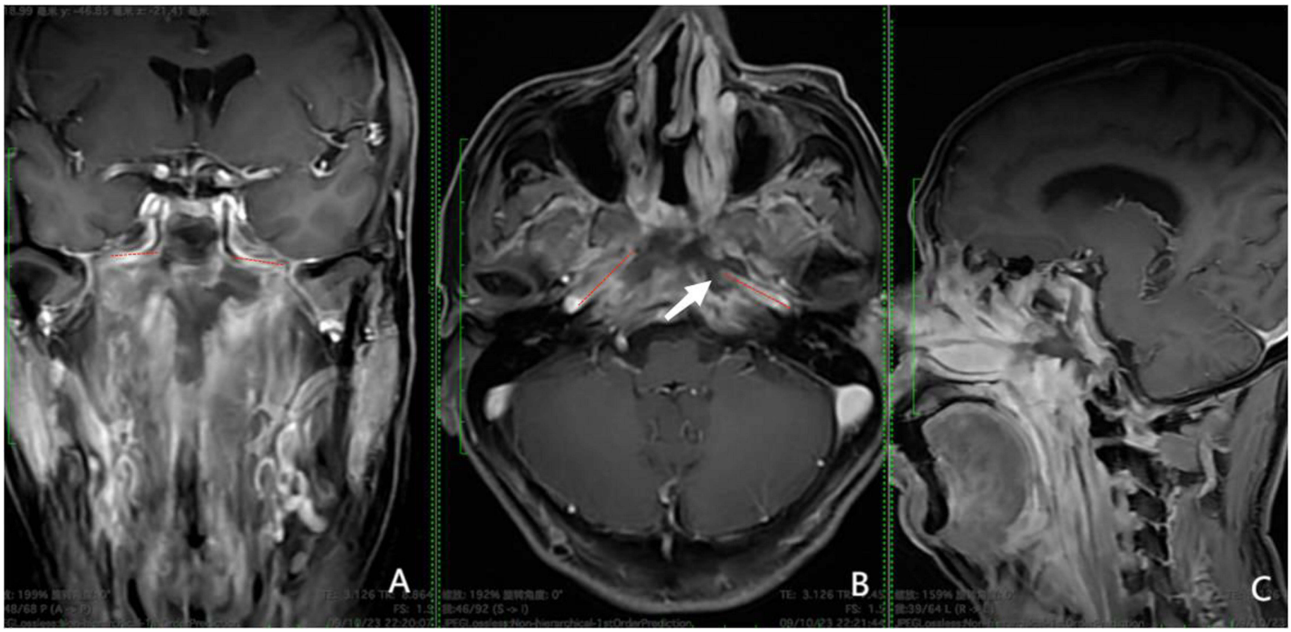

Figure 2 The picture presents an enhanced MRI T1 image that delineates Region B. In this region, while the bone integrity is preserved, there is evident necrosis observable in the area below the petrous apex and around the Lacerum foramen, as indicated by the white arrow. The red dotted line demarcates the horizontal segment of the ICA. (**A**) the coronal plane. (**B**) the axial plane. (**C**) the sagittal plane.

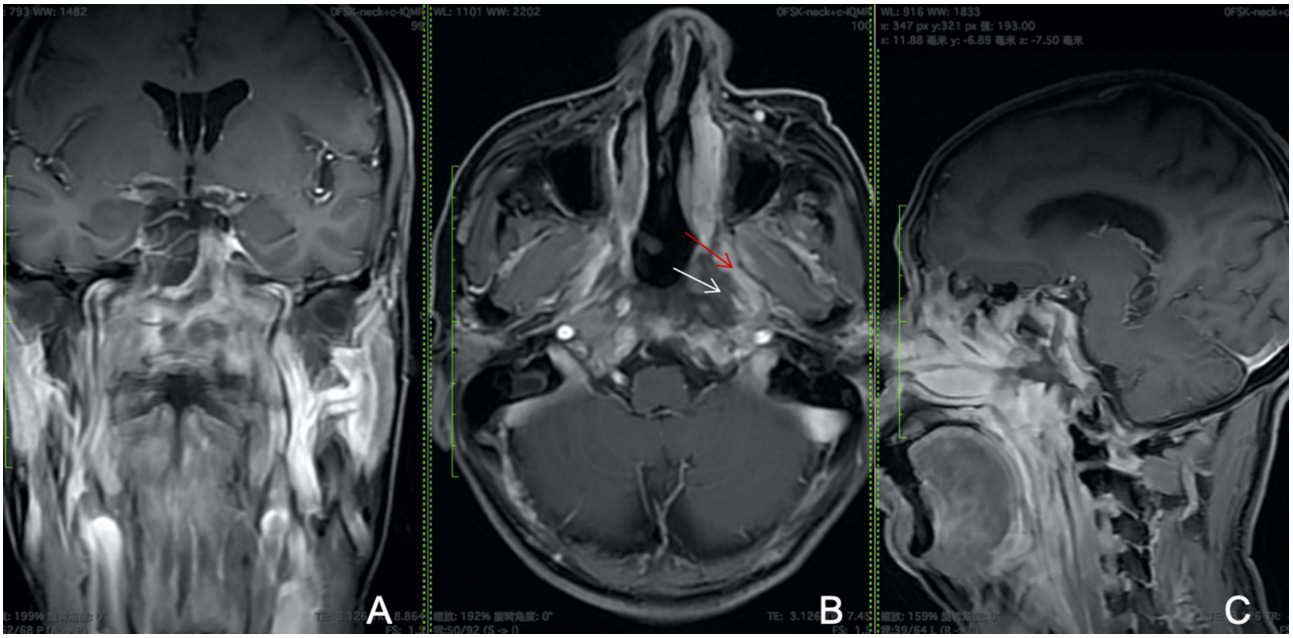

Figure 3 The figure reveals an MRI T1 enhanced image, specifically illustrating the anatomical features of Region D. This region encompasses the external opening of the carotid canal, the area surrounding the eustachian tube, and the muscles involved in palatal movement. Notably, the levator veli palatini muscle is indicated by a red arrow, showing signs of edema, while the tensor veli palatini muscle, marked by a white arrow, exhibits necrosis. (**A**) the coronal plane, (**B**) the axial plane, and (**C**) the sagittal plane.

Statistical Analysis

Categorial variables were transformed into frequencies and percentages. Continuous variables were presented by means and ranges. We compared VRS before and after the surgery by paired-samples Wilcoxon rank-sum test because VRS was ordinal statistics. (version 28.0, Chicago, USA). The statistical test was two-sided, and a P value less than 0.05 was considered statistically significant.

Table 1 Division of Anatomical Regions and Corresponding Anatomical Landmarks

Subregion	Subsegments of the ICA	Anatomical Landmarks
Region A	Paraclival segment	The optic nerve, OCR
Region B	None	Petroclival fissure, jugular foramen, hypoglossal foramen
Region C	Cavernous sinus segment of the ICA	Middle cranial fossa, cavernous sinus, 345 cranial nerve
Region D	Horizontal segment Parapharyngeal segment	VN, mandibular strut, mandibular nerve, external orifice of the ICA

Results

Clinical Characteristics

A total of 19 patients (12 male and 7 female), with a mean age of 53.73 years (range = 32–68 years), were included in this survey. The demographic characteristics of these patients were presented in Table 2. The median follow-up time was 37.47 months (from 2 to 77 months). All patients had no recurrence during the follow-up period. Table 3 presented the post-radiation complications observed in these ORN patients. The average time between the end of radiation therapy and the diagnosis of ORN was 56.8 months (range = 6.8–295.8 months).

Table 2 Demographic and Characteristics of ORN Patients

	N
Number of patients	19
Mean age, years (range)	53.73(32–68)
Mean follow-up time, months (range)	37.47 (2–77)
Sex	
Male	12
Female	7
Primary cancer	
Nonkeratinizing carcinoma of NPC	8
Squamous cell carcinoma of NPC	9
Adenoid cystic carcinoma	1
Squamous cell carcinoma of SS	1
Cancer staging	
III	11
IV	8
Status	
Alive	17
stable	16
recurrence	1
Dead	2

Abbreviations: SS, sphenoid sinus; NPC, nasopharyngeal carcinoma.

Table 3 Post-Radiation Complications

Post-radiotherapy Complication	N
Nasopharynx reflux	16
Dysphagia	5
Lisp	5
Otitis media	3
Choke when drinking	3
Facial paralysis	2
Vestibular dysfunction	1
Sensorineural deafness	1
Secondary hypopituitarism	1
Subclinical hypothyroidism	1
Hypoglossal paralysis	1
Postradiotherapy rhinosinusitis	1
Nasal cavity infection	1

The Effect of the Surgery

1 patient died within 2 months due to a multi-interstitial space infection, and another patient died from the sudden rupture of ICA. The other 17 patients all experienced varying degrees of headache relief. Among them, 16 patients remained stable, while 1 patient experienced a recurrence (Table 2). The patient with ORN recurrence had adenoid cystic carcinoma. Her symptoms improved until 4 years after the initial operation. Sagittal MRI revealed necrosis in the posterior wall of the pharyngeal occipito-atlantal articulation (Figure 4). Therefore, she underwent another sequestrum removal surgery and showed improvement.

At the time of the latest follow-up (mean time 37.47 months), the alleviated rate was 89.4%. The Wilcoxon rank-sum test demonstrated a statistically significant difference in the VRS before and 2 weeks after the surgery ($Z = -3.921$, $P = 0.000$) (Table 4).

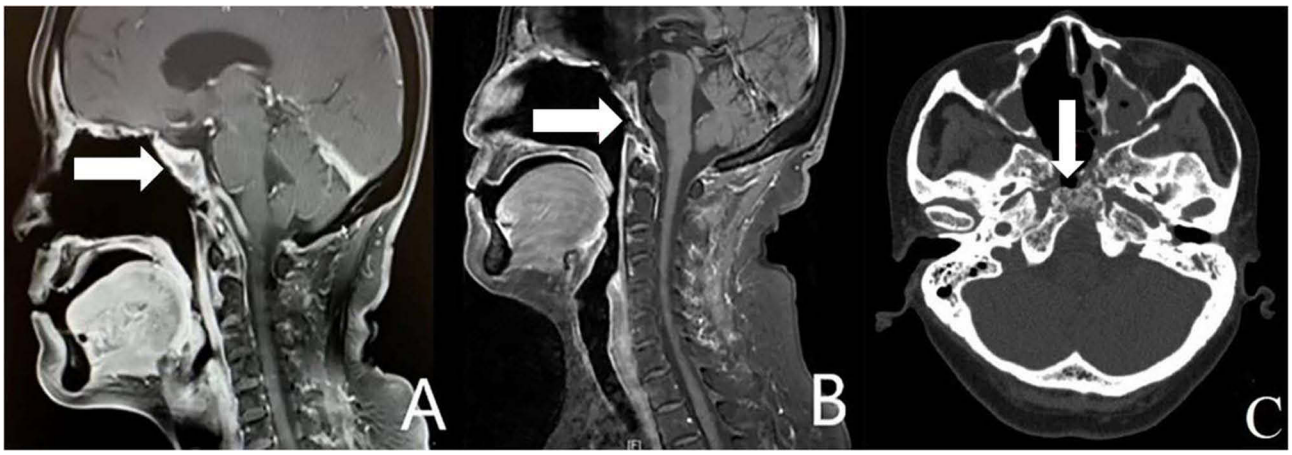

Figure 4 MRI results of the recurrent patient: (**A**) The white arrow shows the midline clivus and superficial mucosa were intensified 2.25 years post operation. There was no obvious necrotic evidence. (**B**) The white arrow shows the recurrent necrosis 4 years after the first surgery (**C**) the white arrow shows the middle line structures are necrotic. The bone matrix around the ICA and clivus shows hypo-intensity.

Table 4 Wilcoxon Rank Sum Test Results

	No Pain	Mild Pain	Moderate Pain	Severe Pain	Z Value	P value
Before the surgery	0	3	14	2	−3.921	0.000
After the surgery	9	10	0	0		

The Clinical Characteristics of SBORN with ICA Involvement

The evidence for determining the involvement of ICA in SBORN is currently unclear. It can be roughly inferred from 3 aspects: symptoms, imaging, and intraoperative exploration.

(1) In terms of symptoms, fatal hemorrhage caused by ICA rupture indirectly proves the involvement. The angiography and embolization of ICA before and after the rupture can provide relevant evidence.
(2) In terms of imaging, abnormal signals in the soft tissue of the affected segment on MRI (Figure 5a), low-density on MRI T1 or non-enhancement on enhanced MRI (Figure 2), or compression and deformation of the lumen (Figure 5a) can indicate the involvement.
(3) Intraoperative anatomical exploration can confirm, such as the formation of pseudoaneurysm (Figure 6).

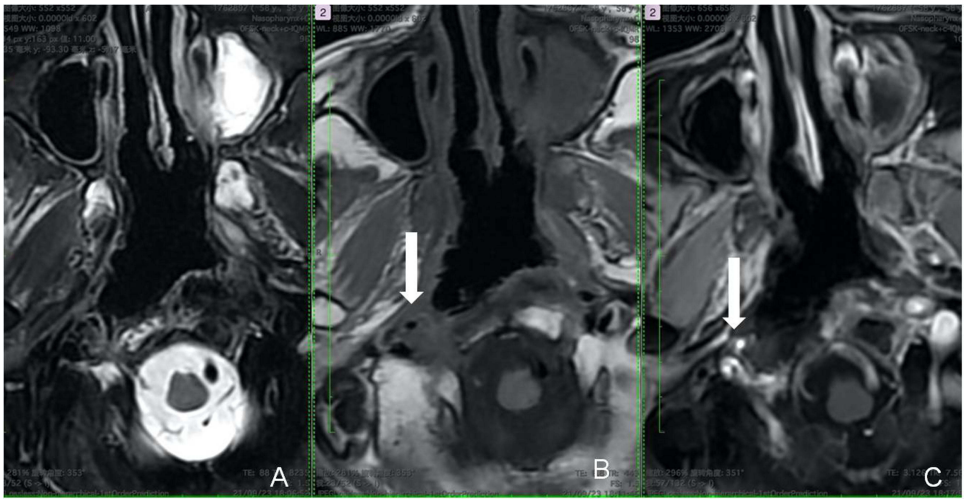

Figure 5 MRI scans (**A**–**C**) reveal the involvement of the adventitia of the right parapharyngeal segments of the ICA (white arrow), which appears compressed and deformed compared to the contralateral internal carotid artery. The T2-weighted MRI (**A**) displays the abnormality in soft tissue composition, while the T1-weighted MRI (**B**) reveals a hypointense adventitia membrane. After gadolinium contrast injection (**C**), enhancement of the adventitia is observed, indicating its involvement in the pathological process.

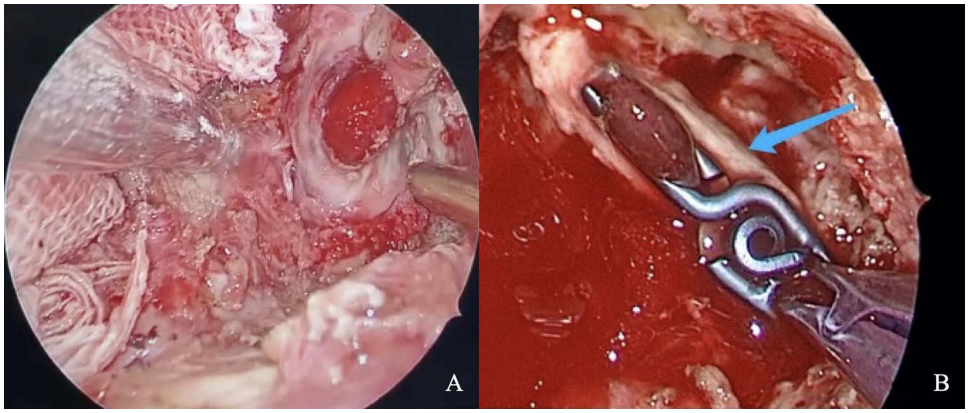

Figure 6 Involvement of the parapharyngeal ICA in a ORN patient leads to the formation of a pseudoaneurysm. (**A**) Intraoperative finding of pseudoaneurysm formation. (**B**) Titanium clips, indicated by the blue arrow, are used to occlude the pseudoaneurysm along the course of the ICA.

Discussion

SBORN is a rare disease that arises as a consequence of radiation therapy and poses significant clinical challenges. This condition is characterized by persistent and debilitating headache, which can severely impact quality of life and survival time. Furthermore, SBORN with ICA invasion poses a considerable risk of rupture and bleeding, which is a leading cause of mortality in these patients. Given the severity and complexity of this condition, precise surgical intervention is widely recognized as the definitive treatment modality for alleviating pain, enhancing quality of life, and prolonging survival time. The importance of timely and accurate diagnosis, along with meticulous surgical planning and execution, cannot be overstated in managing this uncommon but clinically significant disease.

A range of surgical techniques has been described and generally share common principles. These include the thorough removal of necrotic bone debris through drilling until bleeding from the underlying viable bone is observed, and the use of grafts or free flaps for skull base reconstruction. While these approaches are often effective and associated with favorable outcomes, they can be challenged in cases where ICA is involved. However, there is a paucity of literature that provides specific guidance on preoperative planning, surgical management, reconstruction options, and the prevention and treatment of complications in these complex cases. To address this knowledge gap, we conducted a survey utilizing ICA classification system proposed by Dr. Kassam. Our findings suggest that the lacerum foramen and its surrounding area are particularly susceptible to radiation-induced damage, likely due to their proximity to the primary tumor site.

Preoperative evaluation of the location, length, and extent of ICA invasion is essential to prevent iatrogenic injury during surgical intervention. Our institutional protocol follows a structured flowchart (Figure 7). Routine evaluation methods include computed tomography angiography (CTA) and magnetic resonance angiography (MRA), which reveals

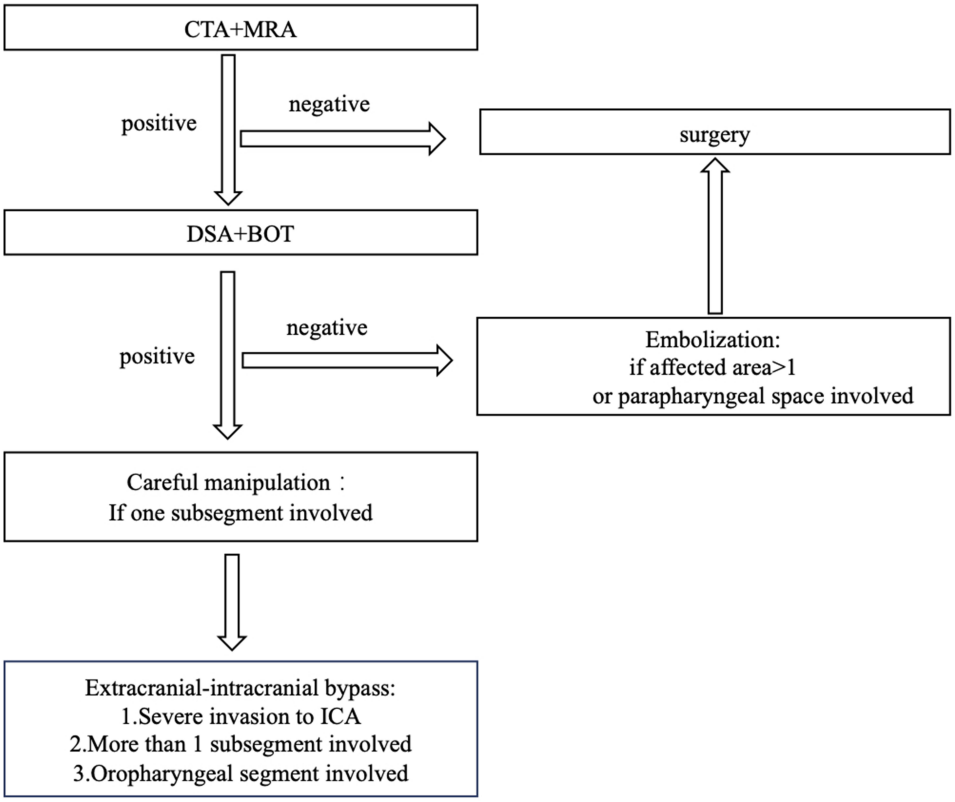

Figure 7 Flow chart for handling involvement: If the DSA and BOT are negative, the surgery can be carried out in a safe manner. However, if there are more than 1 subarea (**A**–**D**) involved, along with invasion of the parapharyngeal space, preoperative embolization is necessary. If the DSA and BOT reveal poor resistance to ischemia and ICA is invaded within a single subsegment, careful manipulation during the surgery can help mitigate the risk of ICA rupture. If there are more than 1 subsegment affected or the oropharyngeal segment is involved, extracranial-intracranial bypass followed by debridement surgery is beneficial. Endovascular stent-graft application can help in dealing with sudden rupture of the ICA, but it is not recommended for treating ICA rupture in such situations.

vascular anatomy and the extent of disease invasion. Additionally, we assess collateral circulation using digital subtraction angiography (DSA) and perform the balloon occlusion test (BOT) to assess cerebral ischemic tolerance.

Exposure of different parts of the invaded artery requires different approaches and techniques. Ultimately, the main principle is to proceed from the farthest to the nearest site, from relatively safe areas to dangerous ones. To ensure the safety of the surgery and precise location of the ICA, reliance on a single anatomical structure is unreliable (Table 5).

Moreover, the Eustachian tube, mandible nerve, and levator veli palatini aid in accurately positioning the parapharyngeal ICA. In our surgical approach, we rely on the clivus recess and maxillary nerve to precisely locate the paraclival segment of the ICA, which lies above the lacerum. By carefully detaching the soft tissue inferiorly, we can identify the intersection between the vidian canal and pterygosphenoidal fissure, which lies in front of the lacerum segment. The Eustachian tube, mandible nerve, mandible strut, petroclival fissure, and sphenopetrosal fissure provide crucial landmarks for tracing the course of the petrous segment, which transitions into the paraclival segment via the lacerum foramen.[17,22–26] We also utilize the maxillary nerve and lingual process of the sphenoid bone to accurately identify the paraclival segment of ICA and the lacerum segment. The meticulous exposure and clear recognition of ICA are critical for safe and effective surgery. The detachment and dissection of necrotic tissue adjacent to the adventitia membrane of the ICA must be performed with great care. In some cases, sterile necrotic tissue may be present and preserved during the surgery.

Finally, it is essential to cover and protect the exposed ICA with a vascularized flap to ensure its long-term survival and to minimize the risk of postoperative complications. When confronted with extensive skull base defects or compromised nasoseptal flaps, the implementation of remote vascularized pedicle flaps, such as the temporoparietal fascia or the temporal musculofascial flap, should be contemplated.[17,22] The choice between a free graft and a vascularized flap in protecting the exposed artery depends on the extension and extent of the bared artery. Submental island flap is commonly used in clinical practice to repair defects of the oropharynx. When necessary, the multilayer reconstruction technique can efficiently reduce the mortality and morbidity of complications. The exposed ICA is protected by pedicled soft tissue on the second layer, together with autologous fat graft from buccal fat pad or infratemporal fossa as substrate. The pedicled tissue with carefully protected supply arteries is of the utmost importance to mucosal flap survival. In the rare event of ICA rupture, we promptly stuff the nasal cavity with a large amount of gauze to control the bleeding, stabilize the patient condition and then transfer them to the angiography suite for endovascular stent-graft insertion. This is a well-established treatment modality that can seal the ruptured vessel and restore blood flow. If the patient is not suitable for endovascular stent-graft insertion, we collaborate with neurosurgeons to perform an extracranial-intracranial bypass surgery. Infection, necrosis, and implant exposure are potential complications, which impacts the patient prognosis and recovery.

Prior to surgery, patients should undergo a comprehensive imaging protocol including CT with contrast, CTA (CT Angiography), CTV (CT Venography), and CTP (CT Perfusion), MRI with contrast enhancement, and MRA (Magnetic Resonance Angiography). These images should be scrutinized to assess for any bone destruction around the internal carotid artery, whether necrosis is adjacent (within 1mm), invading, or encasing the artery, the presence of suspected pseudoaneurysms in the ICA, or any narrowing or even occlusion. For suspected involvement, DSA (Digital Subtraction Angiography) and BOT (Balloon Occlusion Test) should be performed.

Table 5 Useful Landmarks to Locate the ICA

The ICA Classification	Anatomical Landmark
Parapharyngeal ICA	Levator veli palatini, tensor veli palatini, The Eustachian tube, the mandible nerve
Petrous segment	The Eustachian tube, the mandible nerve, mandible strut, petroclival fissure, sphenopetrosal fissure (from external orifice of carotid artery to lacerum foramen)
Lacerum foramen segment	Vidian canal, pterygosphenoidal fissure, lingual process of the sphenoid bone, mandible strut
Paraclival segment	Lacerum foramen, the maxillary nerve, clivus, cavernous sinus

During surgery, based on the anatomical landmarks of the ICA, necrotic tissue should be debrided, and the artery should be exposed and protected. The extent of involvement around the internal carotid artery should also be explored.

For patients who have ICA exposed, regular CTA examinations should be scheduled to assess for the development of pseudoaneurysms and the healing of surrounding flaps. These examinations should be conducted within 24 hours post-surgery, at one week, one month, and three months post-surgery.

The results of our study are encouraging. Apart from 2 deaths, the remaining 17 patients experienced varying degrees of relief, despite the occurrence of some irreversible post-irradiated complications. Several studies have been conducted on this topic worldwide. Ahmed Habib[10] enrolled 31 ORN patients and employed both EEA and open approaches (mandibulectomy or infratemporal fossa resection). The median overall survival (OS), 1-yr OS, and mean recurrence-free survival were 83.9 months, 78.5%, and 89.3 months, respectively. These results align with those of Liu J and Wang DH,[11] who reported a 2-yr OS of 54.2% for 59 patients who underwent SBORN debridement surgery via EEA. Another study[14] included 58 patients who underwent either endoscopic debridement surgery (n=12), maxillary swing operation (n=40), or mandibulotomy (n=6). The mean follow-up time was 36.2 months (range= 2–68 months), and the overall survival rate was 85.2%. Numerous other researchers have also reported surgical outcomes using EEA.[12,13,15,27,28] A recent systematic review[29] found an overall success rate of 77.3%. Our surgical results are similar to these findings.

Conclusion

This study presents a four-quadrant division of SBORN as a standardized and systematic approach to guide surgical intervention for osteoradionecrosis.

Ethic Statement

All clinical records from the study were reviewed under the ethical standards of the institutional research committee-Ethics Committee of Longgang ENT Hospital, Shenzhen (SZLGENTEC2022-0224).

Informed Consent Statement

Informed consent was obtained from all subjects involved in the study.

Disclosure

The authors declare that they have no competing interests.

References

1. Frankart AJ, Frankart MJ, Cervenka B, Tang AL, Krishnan DG, Takiar V. Osteoradionecrosis: exposing the evidence not the bone. *Int J Radiat Oncol Biol Phys*. 2021;109(5):1206–1218. doi:10.1016/j.ijrobp.2020.12.043
2. Marx RE. Osteoradionecrosis: a new concept of its pathophysiology. *J Oral Maxillofac Surg*. 1983;41(5):283–288. doi:10.1016/0278-2391(83)90294-X
3. Raggio BS, Winters R. Modern management of osteoradionecrosis. *Curr Opin Otolaryngol Head Neck Surg*. 2018;26(4):254–259. doi:10.1097/MOO.0000000000000459
4. Chronopoulos A, Zarra T, Ehrenfeld M, Otto S. Osteoradionecrosis of the jaws: definition, epidemiology, staging and clinical and radiological findings. A concise review. *Int Dental J*. 2018;68(1):22–30. doi:10.1111/idj.12318
5. Lee IJ, Koom WS, Lee CG, et al. Risk factors and dose-effect relationship for mandibular osteoradionecrosis in oral and oropharyngeal cancer patients. *Int J Radiat Oncol Biol Phys*. 2009;75(4):1084–1091. doi:10.1016/j.ijrobp.2008.12.052
6. Silvestre-Rangil J, Silvestre FJ. Clinico-therapeutic management of osteoradionecrosis: a literature review and update. *Med Oral Patol Oral Cir Bucal*. 2011;16(7):e900–904. doi:10.4317/medoral.17257
7. Bedwinek JM, Shukovsky LJ, Fletcher GH, Daley TE. Osteonecrosis in patients treated with definitive radiotherapy for squamous cell carcinomas of the oral cavity and naso-and oropharynx. *Radiology*. 1976;119(3):665–667. doi:10.1148/119.3.665
8. King AD, Griffith JF, Abrigo JM, et al. Osteoradionecrosis of the upper cervical spine: MR imaging following radiotherapy for nasopharyngeal carcinoma. *Eur. J. Radiol.* 2010;73(3):629–635. doi:10.1016/j.ejrad.2008.12.016
9. Lalani N, Huang SH, Rotstein C, Yu E, Irish J, O'Sullivan B. Skull base or cervical vertebral osteomyelitis following chemoradiotherapy for pharyngeal carcinoma: a serious but treatable complication. *Clin Transl Radiat Oncol*. 2018;8:40–44. doi:10.1016/j.ctro.2017.11.005
10. Habib A, Hanasono MM, DeMonte F, et al. Surgical Management of Skull Base Osteoradionecrosis in the Cancer Population - Treatment Outcomes and Predictors of Recurrence: a Case Series. *Operative Neurosurg*. 2020;19(4):364–374. doi:10.1093/ons/opaa082
11. Liu J, Ning X, Sun X, Lu H, Gu Y, Wang D. Endoscopic sequestrectomy for skull base osteoradionecrosis in nasopharyngeal carcinoma patients: a 10year experience. *Int J Clin Oncol*. 2019;24(3):248–255. doi:10.1007/s10147-018-1354-8

12. Zhang H, Gao KL, Xie ZH, et al. [Clinical study on endoscopic surgery for soft tissue necrosis of cranial base after radiotherapy for nasopharyngeal carcinoma]. *Zhonghua Er Bi Yan Hou Tou Jing Wai Ke Za Zhi = Chinese Journal of Otorhinolaryngology Head and Neck Surgery*. 2021;56(1):26–32. doi:10.3760/cma.j.cn115330-20200608-00483
13. Chen Z, Qiu QH, Zhan JB, Zhu ZC, Peng Y, Liu H. [Endoscopic surgery and reconstruction for extensive osteoradionecrosis of skull base after radiotherapy for nasopharyngeal carcinoma]. *Zhonghua Er Bi Yan Hou Tou Jing Wai Ke Za Zhi = Chinese Journal of Otorhinolaryngology Head and Neck Surgery*. 2016;51(12):881–886. doi:10.3760/cma.j.issn.1673-0860.2016.12.001
14. Huang WB, Wong STS, Chan JYW. Role of surgery in the treatment of osteoradionecrosis and its complications after radiotherapy for nasopharyngeal carcinoma. *Head Neck*. 2018;40(2):369–376. doi:10.1002/hed.24973
15. Lin F, Yu Y, Chen W, et al. [Clinical classification of osteoradionecrosis of temporal bone and the treatment of massive osteonecrosis]. *Lin Chuang Er Bi Yan Hou Tou Jing Wai Ke Za Zhi = Journal of Clinical Otorhinolaryngology, Head, and Neck Surgery*. 2012;26(1):1–4. doi:10.13201/j.issn.1001-1781.2012.01.004
16. Huang XM, Zheng YQ, Zhang XM, et al. Diagnosis and management of skull base osteoradionecrosis after radiotherapy for nasopharyngeal carcinoma. *Laryngoscope*. 2006;116(9):1626–1631. doi:10.1097/01.mlg.0000230435.71328.b9
17. Labib MA, Prevedello DM, Carrau R, et al. A road map to the internal carotid artery in expanded endoscopic endonasal approaches to the ventral cranial base. *Neurosurgery*. 2014;10(Suppl 3):448–471. doi:10.1227/NEU.0000000000000362
18. Ferreira-Valente MA, Pais-Ribeiro JL, Jensen MP. Validity of four pain intensity rating scales. *Pain*. 2011;152(10):2399–2404. doi:10.1016/j.pain.2011.07.005
19. Zhou B, Huang Q, Sun J, et al. Resection of inverted papilloma of the maxillary sinus via a prelacrimal recess approach: a multicenter retrospective analysis of surgical efficacy. *Am J Rhinol Aller*. 2018;32(6):518–525. doi:10.1177/1945892418801243
20. Zhou B, Han DM, Cui SJ, Huang Q, Wang CS. Intranasal endoscopic prelacrimal recess approach to maxillary sinus. *Chinese Med J*. 2013;126(7):1276–1280. doi:10.3760/cma.j.issn.0366-6999.20121754
21. Hadad G, Bassagasteguy L, Carrau RL, et al. A novel reconstructive technique after endoscopic expanded endonasal approaches: vascular pedicle nasoseptal flap. *Laryngoscope*. 2006;116(10):1882–1886. doi:10.1097/01.mlg.0000234933.37779.e4
22. Abdulrauf SI, Ashour AM, Marvin E, et al. Propose d clinical internal carotid artery classification system. *J Craniovertebral Junction & Spine*. 2016;7(3):161–170. doi:10.4103/0974-8237.188412
23. Rivera-Serrano CM, Terre-Falcon R, Fernandez-Miranda J, et al. Endoscopic endonasal dissection of the pterygopalatine fossa, infratemporal fossa, and post-styloid compartment. Anatomical relationships and importance of eustachian tube in the endoscopic skull base surgery. 2010. *Laryngoscope*. 120. Suppl 4:S244.
24. Patel CR, Fernandez-Miranda JC, Wang WH, Wang EW. Skull Base Anatomy. *Otolaryngologic Clin North Am*. 2016;49(1):9–20. doi:10.1016/j.otc.2015.09.001
25. Li W, Chae R, Rubio RR, et al. Characterization of anatomical landmarks for exposing the internal carotid artery in the infratemporal fossa through an endoscopic transmasticator approach: a morphometric cadaveric study. *World Neurosurg*. 2019;131:e415–e424. doi:10.1016/j.wneu.2019.07.185
26. Xu X, Ong YK. An endoscopic anatomical study of the levator veli palatini and its relationship to the parapharyngeal internal carotid artery. *Head Neck*. 2020;42(8):1829–1836. doi:10.1002/hed.26101
27. Han P, Wang X, Liang F, et al. Osteoradionecrosis of the Skull Base in Nasopharyngeal Carcinoma: incidence and Risk Factors. *Int J Radiat Oncol Biol Phys*. 2018;102(3):552–555. doi:10.1016/j.ijrobp.2018.06.027
28. Lee CC, Ho CY. Post-treatment late complications of nasopharyngeal carcinoma. *Eur Arch Otorhinolaryngol*. 2012;269(11):2401–2409. doi:10.1007/s00405-011-1922-2
29. Shaikh N, Makary CA, Ryan L, Reyes C. Treatment outcomes for osteoradionecrosis of the central skull base: a systematic review. *J Neurol Surg Part B*. 2022;83(Suppl 2):e521–e529. doi:10.1055/s-0041-1733973